JOURNAL OF AGRICULTURAL AND FOOD CHEMISTRY

Enzymatic Hydrolysis as a Means of Expanding the Cold Gelation Conditions of Soy Proteins

BAS J. H. KUIPERS,[†,§] GERRIT A. VAN KONINGSVELD,[†,§] ARNO C. ALTING,[#] FRANK DRIEHUIS,[#] HARRY GRUPPEN,[†,§] AND ALPHONS G. J. VORAGEN*[,†,§]

Centre for Protein Technology, Wageningen, The Netherlands; Department of Agrotechnology and Food Sciences, Laboratory of Food Chemistry, Wageningen University, P.O. Box 8129, 6700 EV Wageningen, The Netherlands; and NIZO food research, Ede, The Netherlands

Acid-induced cold gelation of soy protein hydrolysates was studied. Hydrolysates with degrees of hydrolysis (DH) of up to 10% were prepared by using subtilisin Carlsberg. The enzyme was inhibited to uncouple the hydrolysis from the subsequent gelation; the latter was induced by the addition of glucono-δ-lactone. Visual observations, confocal scanning laser microscopy images, and the elasticity modulus showed that hydrolysates gelled at higher pH values with increasing DH. The nonhydrolyzed soy protein isolate gelled at pH ~6.0, whereas a DH = 5% hydrolysate gelled at pH ~7.6. Gels made from hydrolysates had a softer texture when manually disrupted and showed syneresis below a pH of 5−5.5. Monitoring of gelation by measuring the development of the storage modulus could be replaced by measuring the pH onset of aggregate formation ($pH_{Aggr-onset}$) using turbidity measurements. The rate of acidification was observed to also influence this $pH_{Aggr-onset}$. Changes in ionic strength (0.03, 0.2, and 0.5 M) had only a minor influence on the $pH_{Aggr-onset}$, indicating that the aggregation is not simply a balance between repulsive electrostatic and attractive hydrophobic interactions, but is much more complex.

KEYWORDS: Aggregation; coagulation; proteolysis; enzymatic hydrolysis; soy protein isolate; subtilisin Carlsberg; cold gelation

INTRODUCTION

Soy proteins are used in the food industry for their ability to form heat-induced gels (*1*). This gelation involves the formation of aggregates, which subsequently form a more or less continuous network. The properties of heat-induced gels depend on the conditions during aggregate formation, such as protein concentration, temperature and duration of heat treatment, ionic strength, and pH (*2*, *3*). Gels can also be prepared at ambient temperature, as reviewed by Bryant and McClements (*4*). In this so-called cold gelation process two stages can be distinguished: (i) the preparation of a heat-denatured globular protein solution and (ii) the induction of gelation at ambient temperature. Using heat-denatured soy proteins, gelation can be induced by gradual acidification (*5*). When the pH is lowered toward the isoelectric point, the electrostatic repulsion between proteins decreases (*6*), which results in a turbid gel due to random aggregation of the proteins (*7*). Upon lactic acid fermentation, during which sugars are metabolized into lactic acid, the pH decreases gradually, eventually resulting in the formation of a gel when the isoelectric pH of the protein is approached. This gel formation can be studied in the absence of acid-producing microorganisms, by the use of glucono-δ-lactone (GDL) (*8*). Because GDL is water-soluble and slowly hydrolyzes into gluconic acid, its addition results in a gradual and homogeneous decrease in pH without the need for stirring. This is in contrast to acidification by the addition of organic or inorganic acids, which requires mixing during acidification, resulting in inhomogeneous gel formation.

In addition to heating and acidification, enzymatic hydrolysis can be used to improve the functional properties of proteins (*9*). In general, hydrolysis is assumed to be unfavorable for the gelling properties of proteins, because it increases the number of charged groups and reduces the molecular weight, which hamper gelation (*10*). On the other hand, the structure of the protein is altered during hydrolysis, and buried hydrophobic groups become exposed, which might result in aggregate formation. Under certain conditions these aggregates can form gel networks, and in some cases, hydrolysis has been observed to enhance the gelling properties of the protein (*11*−*14*).

Limited hydrolysis of whey proteins by *Bacillus licheniformis* protease (BLP) was shown to result in an increased gel strength after heating of hydrolysates at neutral pH (*11*). Doucet et al. (*13*) and Otte et al. (*14*) observed that during extensive hydrolysis of bovine whey proteins with Alcalase and limited hydrolysis with BLP, respectively, gels were formed. For soy

* Author to whom correspondence should be addressed (telephone +31 317 483209; fax +31 317 484893; e-mail fons.voragen@wur.nl).
† Centre for Protein Technology.
§ Wageningen University.
# NIZO food research.

10.1021/jf048622h CCC: $30.25
Published on Web 01/21/2005

proteins it was found that by the action of bromelain gelation could be induced (*12*). It has also been shown that different, mainly alkaline and neutral, proteinases of microbial origin can induce coagulation of proteins in soy milk (*15*). In accordance with this, Inouye (*16*) recently reported that subtilisin Carlsberg is able to induce aggregation during the hydrolysis of soy protein isolates, but gelling properties were not studied. It might be expected that under certain conditions these aggregates would form a gel network upon hydrolysis. Because the hydrolysis of soy proteins can take place at ambient temperature, hydrolysis may be a way to modulate the structure of soy proteins to improve their performance in the cold gelation process. To be able to modulate the texture of soy protein products, the aggregation behavior of the protein hydrolysates and the parameters that influence this behavior, such as the degree of hydrolysis (DH), pH, and ionic strength, should be understood. To our knowledge no detailed information is available on the influence of these parameters on the gelation of soy protein hydrolysates.

The purpose of this study was, therefore, to investigate the influence of DH, pH, and ionic strength on the aggregation and gelation behavior of soy protein hydrolysates, made with subtilisin Carlsberg at ambient temperature. In particular, subtilisin Carlsberg was chosen because it is the main enzyme in Alcalase, which is a commercially available, food-grade, industrial enzyme mixture (*17*).

MATERIALS AND METHODS

Materials and Chemicals. Hyland soybeans (non-GMO) were supplied by Fa. L. I. Frank (Twello, The Netherlands). Subtilisin Carlsberg from *B. licheniformis* [10 units/mg of solid: 1 unit releases color, equivalent to 1.0 μmol (181 μg) of tyrosine per minute from casein at pH 7.5 at 37 °C as measured using the Folin−Ciocalteu reagent], GDL, and phenylmethanesulfonyl fluoride (PMSF) were obtained from Sigma Chemical Co. (St. Louis, MO; articles P-5380, P-7626, and G-4750, respectively). All other chemicals were of analytical grade and were purchased from Merck (Darmstadt, Germany).

Analysis of Protein Content. The nitrogen content of various samples was estimated according to the Dumas method using an NA2100 nitrogen and protein analyzer (CE Instruments, Milan, Italy) according to the manufacturer's instructions. Methionine was used as a standard. Nitrogen content was multiplied by 5.71 to calculate the protein content (*18*).

Preparation of Soy Protein Isolate (SPI). Soybean meal (SBM) was prepared by crushing soybeans with a Condux-Werk LV 15M (Condux-Werk, Wolfgang bei Hanau, Germany), followed by milling the crushed beans in a Fritsch Pulverisette 14702 using a 0.5 mm sieve (Fritsch Gmb, Albisheim, Germany). Milling was performed in the presence of solid CO_2 to prevent excessive heating (volume ratio of soybean to CO_2 was approximately 4:1). The SBM was defatted three times with hexane at room temperature (w/v ratio of SBM/hexane = 1:10) followed by drying to the air.

To obtain the SPI, the defatted SBM was suspended in a 30 mM Tris-HCl buffer, pH 8, containing 10 mM 2-mercaptoethanol and stirred at ambient temperature for 1.5 h (w/v ratio of SBM/buffer = 1:10). After removal of the insoluble parts by centrifugation (30 min, 12000*g*, 10 °C), the supernatant was brought to pH 4.8 with 2 M HCl to induce precipitation of the proteins. After 2 h at room temperature, the dispersion was centrifuged (20 min, 12000*g*, 10 °C). The precipitate was washed twice with Millipore water (approximate v/v ratio precipitate/water = 1:9) followed by suspending it in water and adjusting its pH to 8 before it was freeze-dried. The protein content (N × 5.71) of the freeze-dried SPI was 83.3 (±1.6)% (w/w).

Heat Denaturation of SPI. Prior to each hydrolysis experiment, an SPI solution was freshly prepared by suspending the freeze-dried SPI in Millipore water containing 0.032% (w/v) sodium azide to a concentration of 8% (w/w) (6.7% w/w protein). If necessary, the pH was adjusted to 8 with 2 M NaOH. The dispersion was stirred overnight at 4 °C. After equilibration to ambient temperature, the pH was readjusted to 8, if necessary. The slightly turbid solution was subsequently centrifuged (30 min, 22000*g*, 20 °C), and the supernatant was heated in a water bath at 95 °C for 30 min in a closed bottle, followed by immediate cooling in a water bath at room temperature. To determine whether the heating step of the SPI solution was sufficient to irreversibly denature the proteins, DSC experiments were performed on a VP-DSC microcalorimeter (MicroCal Inc., Northampton, MA). DSC experiments were conducted with the SPI solution before and after the heat treatment (30 min, 95 °C). The SPI solutions were diluted to a protein concentration of ∼5 mg/mL with 10 mM potassium phosphate buffer, pH 7.6, containing 0.5 M NaCl. Thermograms were recorded from 20 to 105 °C with a heating rate of 1 K/min. The nonheated SPI showed two endothermic transitions at about 79 and 95 °C, representing the denaturation of β-conglycinin and glycinin, respectively (*19*). The heated SPI showed no endothermic effect. The heated SPI solution, which will further be denoted SPI solution (DH = 0%), had a clear, slightly opaque appearance and had a protein concentration of 6.2 ± 0.1% (w/w).

Proteolysis of SPI. Hydrolysates with various DH values (percentage of peptide bonds cleaved; 1.3, 2.5, 3.8, 5.0, 6.3, 7.5, and 10.0%) were prepared from the SPI solution by hydrolysis at pH 8 and 40 °C using subtilisin Carlsberg. Hydrolysates were freshly prepared prior to each experiment. The pH and DH were controlled using the pH-stat method by using a 719S Titrino (Metrohm Ion Analysis, Herisau, Switzerland) (*20*). The enzyme concentration varied from 3 to 6 units/g of substrate, whereas the molarity of the NaOH solution used to maintain the pH varied from 0.1 to 0.5 M. The higher the desired DH was, the higher the amount of enzyme and the higher the molarity of NaOH that was used. The enzyme was dissolved in Millipore water and directly added to the SPI solution. When the desired DH was reached, the enzymatic hydrolysis was stopped (*21*) by the addition of a 100 mM PMSF stock solution in 2-propanol to a final concentration of 1 mM. Instability of the PMSF in aqueous solutions (*22*) resulted in a slight decrease in pH directly after addition. Approximately 10 min after PMSF addition, the pH was stable, and the hydrolysate was cooled to room temperature. Although PMSF did not inhibit subtilisin Carlsberg completely, the effect of the remaining activity was negligible for the time scales used in all experiments, as tested by size exclusion chromatography. The average hydrolysis time was ∼30 min. At DH values below 10%, the hydrolysates had an appearance similar to that of the heated SPI solution. During more extensive hydrolysis (DH ≥ 10%), however, the solution became turbid.

Preparation of Cold-Set Gels. Gels were prepared from the SPI solution and the hydrolysates thereof, by the addition of GDL, which was freshly dissolved in ice water before each experiment. Two different gels were prepared from each sample, one with a final pH of 5.2 (±0.2) and the other with a final pH of 3.1 (±0.1), by adding 0.45−0.6 and 5−6% (w/w) GDL, respectively. The buffering capacity of the hydrolysates increased with increasing DH and, therefore, more GDL was added at the higher DH values.

To correct for the different amounts of NaOH added during hydrolysis, the ionic strength and the protein concentration in the gels were standardized by the addition of NaCl solution (2 or 5 M) and/or Millipore water before all further experiments. The final protein content of the gels was ∼4.0% w/w with ionic strengths of 0.03, 0.2, or 0.5 M.

Confocal Scanning Laser Microscopy (CSLM). Imaging was carried out of gels made from the SPI solution and hydrolysates with a DH of 2.5 and 5.0%, all at an ionic strength of 0.03 M. A confocal scanning laser microscope type TCS-SP (Leica Microsystems AG, Wetzlar, Germany), configured with an ArKr laser for single-photon excitation (JDS Uniphase, San Jose, CA), was used. By adding increasing amounts of GDL, gels with various final pH values (pH 5−8) were obtained. The protein gels were stained by applying 10 μL of a 0.2% (w/v) Rhodamine B solution to 1 mL of gel. The 568 nm laser line was used for excitation to induce a fluorescent emission of Rhodamine B, which was monitored between 600 and 700 nm. The pore size and area percent covered by pores on the picture were estimated using Leica Qwin software (Leica Microsystems AG). Directly after the picture was made, the gel was disrupted and the pH

was measured using a Metrohm Biotrode micro pH glass electrode (Metrohm Ion Analysis, Herisau, Switzerland).

Turbidity Experiments. Aggregate formation in the samples during the GDL acidification was followed as described by Alting and coworkers (*23*), by measuring the turbidity as the absorbance at 500 nm at 25 °C on a Cary 1E UV−vis spectrophotometer (Varian Nederland BV, Houten, The Netherlands) equipped with a temperature controller. The pH was monitored simultaneously in samples placed in a water bath at 25 °C. Samples were measured in glass cuvettes with a path length of 1 mm to prevent sedimentation. The parallel measurement of the pH as a function of time allowed us to monitor the turbidity as a function of pH at various DH values (0, 1.3, 2.5, 3.7, 5.0, and 6.2%) and ionic strengths (0.03, 0.2, and 0.5 M).

Rheological Characterization of Gels. The formation of a gel network in SPI solutions with DH values of 0, 2.5, and 5.0% (I = 0.03 M) was followed by simultaneously monitoring the storage modulus (G'), the turbidity, and the pH as a function of time at 25 °C. Small-amplitude oscillatory measurements were made with a Carri-Med CLS^2 500 rheometer (TA Instruments, New Castle, DE) using a double-walled-cylinder measuring unit (R_1, R_2, R_3, R_4, and h are 20, 20.38, 21.96, 22.38, and 20.5 mm, respectively). Immediately after the addition of GDL, samples were brought into the measuring unit and covered with a thin layer of paraffin oil to prevent evaporation. All experiments were conducted in oscillation at a strain of 1% and a frequency of 1 Hz. The strain was within the linear region.

Light Scattering. Dynamic light-scattering experiments were done using a Malvern Autosizer IIC Submicron particle size distribution analyzer (Malvern Instruments Ltd., Worcestershire, U.K.). The system consisted of a Malvern PCS41 optics unit with a 5 mW He−Ne laser and a Malvern K7032-ES correlator used in serial configuration. The Autosizer IIC worked at a fixed scattering angle of 90°, and the wavelength of the laser beam was 632.8 nm, resulting in a wave vector of 0.0187 nm^{-1}. Hydrolysates were diluted with 20 mM Tris-HCl buffer, pH 8.15, resulting in a protein concentration of ~20 mg/mL, before being transferred to 10 mm quartz cuvettes. The average apparent diameter of the protein aggregates was monitored at 20 (±0.1) °C. The Malvern software was used in "Easy Mode", which means that the interval time was automatically adjusted to the "optimal" value. The apparent diameter of the particles in solution was calculated from a cumulant fit of the intensity autocorrelation function (*24*). Aggregate sizes were estimated at least in triplicate.

High-Performance Size Exclusion Chromatography (HP-SEC). Aliquots (300 μL) of SPI solution and hydrolysate solutions (~10 mg of protein/mL) were mixed with 510 μL of 0.15 M Tris-HCl buffer, pH 8, containing 100 mM 1,4-dithiothreitol (DTT) and 8 M guanidinium chloride. After 1 h of stirring at ambient temperature, 310 μL of acetonitrile and 200 μL of 8 M guanidinium chloride, containing 2% (v/v) trifluoroacetic acid (TFA), were added, and the mixture was stirred for another 1 h. After centrifugation (15 min, 22000*g*, 20 °C), the supernatants were applied to a Shodex Protein KW-803 column (300 × 8 mm; Showa Denko K.K., Tokyo, Japan). The column was equilibrated with 40% (v/v) aqueous acetonitrile containing 0.1% (v/v) TFA. The flow rate was 0.6 mL/min, and the absorbance of the eluate was monitored at 220 nm. According to the manufacturer's specification, the void volume of the column was ~5.7 mL. The included volume was estimated using GlyTyr (238 Da) and was observed to be ~12.4 mL. For the SPI solution separate fractions were collected and dried in an ALPHA-RVC CMC-1 rotating vacuum concentrator (Martin Christ, Osterode am Harz, Germany) followed by analysis by gel electrophoresis.

Gel Electrophoresis. The protein composition of SPI, hydrolysates of various DH values, and the various fractions of SPI collected during HP-SEC was determined using SDS-PAGE under reducing conditions (10 mM 2-mercaptoethanol) on a Mini-protean II system (Bio-Rad Laboratories, Richmond, CA) according to the instructions of the manufacturer. Gels (12%) were calibrated with marker proteins with molecular masses ranging from 14.4 to 94 kDa (Amersham Biosciences, Roosendaal, The Netherlands) and were stained with Coomassie Brilliant Blue.

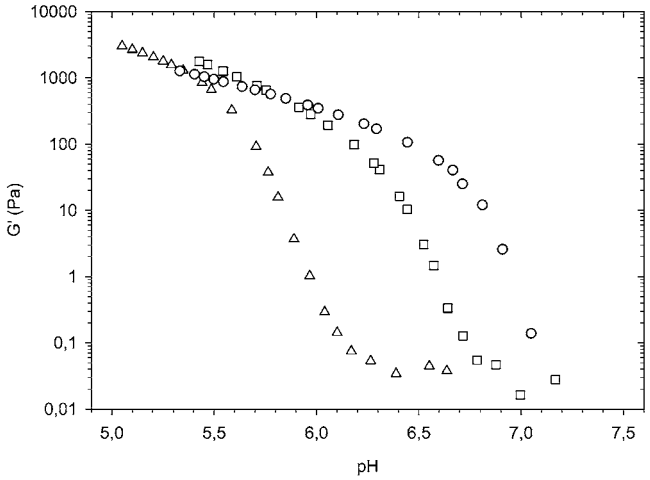

Figure 1. Development of the storage modulus (G') as a function of pH for DH = 0% (△), 2.5% (□), and 5.0% (○) at I = 0.03 M.

RESULTS

Cold Gelation of Hydrolysates. Gels of the SPI solution and hydrolysates thereof with various DH values were made by gradual acidification. When the pH was lowered from 8, one of the most striking effects was the observation that the higher the DH of the hydrolysates, the higher the pH at which gelation started. Just below this gelation pH the gels had an opaque appearance, which became more turbid upon further pH decrease. Around pH 5 syneresis could be observed in gels made from the hydrolysates, whereas in gels from SPI no syneresis was observed. Compared to gels made from SPI, gels made from hydrolysates could be disrupted more easily.

In **Figure 1** the storage modulus as function of pH is presented for DH = 0, 2.5, and 5.0% samples at I = 0.03 M. Because of syneresis, this experiment was not carried out at pH values <5. When the pH of the DH 0, 2.5, and 5.0% solutions is lowered, G' starts to increase at pH 6.3, 6.8, and 7.2, respectively. This confirms the visual observations described above. The maximum G' values were in the range of 1000−3000 Pa.

CSLM of Cold-Gelled Hydrolysates. The microstructures of the cold-set gels were subsequently characterized by CSLM. **Figure 2** shows the CSLM images of the gels prepared from SPI solutions with a DH of 0, 2.5, and 5.0%, made at 16 h after the addition of GDL. The orange parts represent protein-bound Rhodamine, whereas the dark spots represent places where little or no protein is present, which can be assumed to be pores in the protein gel network. Visual observations, the area percent covered by the pores, and the average pore diameter of the gels corresponding to the images shown in **Figure 2** are presented in **Table 1**. When **Figure 2** is compared with **Table 1**, the visual observations show that conditions at which no gel was formed coincided with a homogeneous distribution of the proteins. When the formation of gels was observed, this coincided with the formation of a network, observed as the appearance of pores. These pores increased in average size with decreasing pH. The development of the total area percent covered by pores showed the same trend (**Table 1**).

When samples at one DH value are compared, it can be observed that a coarser network is formed with decreasing pH, for all three DH values (**Figure 2**). At DH = 5.0%, for example, no pores were observed at pH 8.1, whereas at pH 7.6 very small pores, with an average pore diameter of 0.22 μm, were observed. At pH 6.9 the pores became much more abundant and had an average diameter of 0.56 μm. The largest pores, with an average

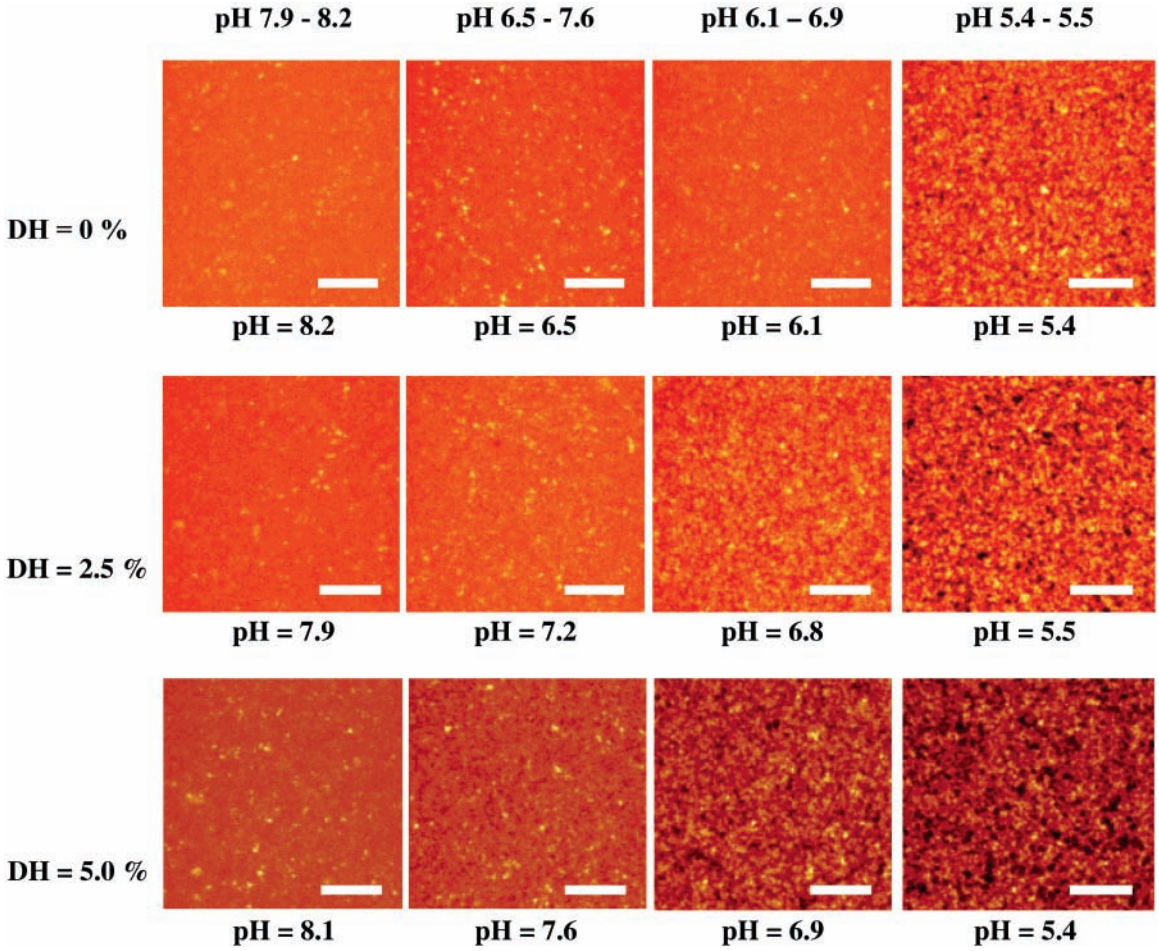

Figure 2. CSLM images of 4.0% (w/w) protein gels prepared from SPI solutions with a DH of 0, 2.5, and 5.0% (I = 0.03 M). The bars represent a length of 10 μm. The pH values of the gels are presented at the bottom of each image.

Table 1. Characteristics of the CSLM Images As Presented in **Figure 2** of 4.0 % (w/w) Protein Gels Prepared from SPI Solutions with a DH of 0, 2.5, and 5.0 % (I = 0.03 M)

		pH 7.9–8.2	pH 6.5–7.6	pH 6.1–6.9	pH 5.4–5.5
DH = 0%	visual observation	liquid	liquid	liquid	turbid gel
	% area covered by pores	0.1	0.1	0.1	7.2
	average pore diameter (μm)	0.20 (±0.01)[a]	0.20 (±0.01)[a]	0.20 (±0.01)[a]	0.44 (±0.23)
DH = 2.5%	visual observation	liquid	liquid	opaque gel	turbid gel
	% area covered by pores	0.1	0.1	2.4	12.5
	average pore diameter (μm)	0.20 (±0.01)[a]	0.20 (±0.04)[a]	0.33 (±0.16)	0.57 (±0.33)
DH = 5.0%	visual observation	liquid	opaque gel	turbid gel	turbid gel[b]
	% area covered by pores	0.1	0.5	11.1	13.1
	average pore diameter (μm)	0.20 (±0.01)[a]	0.22 (±0.05)	0.56 (±0.35)	0.69 (±0.42)

[a] The minimum pore size that can be measured is 0.2 μm. [b] Syneresis was observed in this sample.

diameter of 0.69 μm, were observed at pH 5.4 at DH = 5.0%. In this sample syneresis was also observed.

When samples at a fixed pH (**Figure 2**) are compared, the network seems to become coarser with increasing DH. This is confirmed by the data in **Table 1**, which show that at pH 5.4/5.5 the average pore diameter increases from 0.44 to 0.69 μm, when the DH is increasing from 0 to 5.0%.

Turbidity of Cold-Gelled Hydrolysates. Aggregate formation often precedes gelation and can be monitored in acid-induced gels as an increase in turbidity, because gels that are formed around the pI of the protein usually consist of large random aggregates and often result in a coarse protein network (*25*, *26*). Turbidity measurements were therefore used as a tool to study gel formation indirectly, with the advantage that different measurements could be performed simultaneously. Experiments were performed at various ionic strengths to obtain information about the contribution of electrostatic interactions in the aggregation process. The absorbance at 500 nm as a function of pH for DH 0, 2.5, and 5.0% at I = 0.03, 0.2, and 0.5 M is shown in **Figure 3**.

At all of the conditions used it was observed that with decreasing pH the turbidity started to increase at a specific pH, which indicates that at these conditions aggregates were formed. The development of the turbidity as a function of pH followed a kind of S-curve until a maximum was reached. The pH at which aggregates start to form is denoted the pH of aggregation onset ($pH_{Aggr-onset}$), which is defined as the intersection of the tangent at the point of inflection of the S-curve with the x-axis.

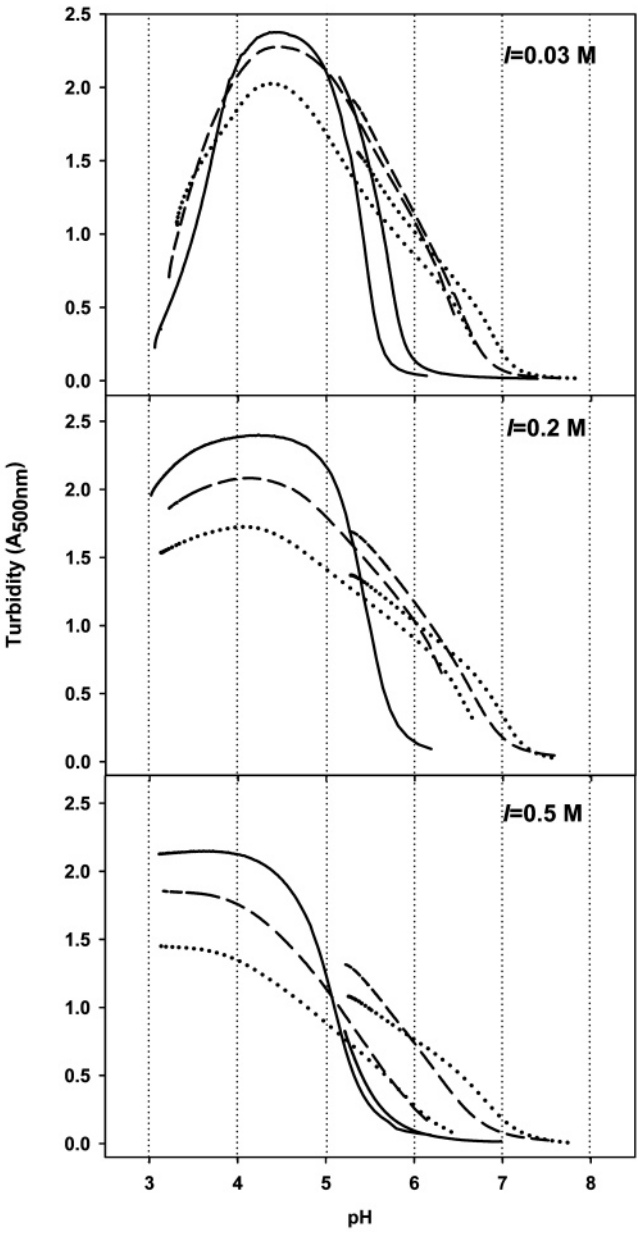

Figure 3. Turbidity at 500 nm for DH = 0% (–), 2.5% (– –), and 5.0% (···) as a function of pH at $I = 0.03$, 0.2, and 0.5 M.

If turbidity is studied over a pH range from 3 to 8, the amount of GDL used to reach pH 3 results in too high a rate of acidification in the pH 5−8 range. Therefore, also a gel was prepared of the same SPI solution or hydrolysate, using a lower amount of GDL. The curves obtained of one hydrolysate using two different levels of GDL did not follow the same course (**Figure 3**), indicating that the rate of acidification affects the aggregation process. At a particular pH, the turbidity of the slowly acidified sample was higher compared to that of the quickly acidified sample; a low rate of acidification gives the proteins more time to aggregate.

The curves at $I = 0.03$ M reached a maximum in turbidity at pH ~4.5, which was followed by a decrease in turbidity below pH 4.5. The turbidity maximum decreased with increasing DH (**Figure 3**), whereas the pH of maximum turbidity remained constant. With increasing DH, the $pH_{Aggr-onset}$ increased to 5.9, 6.9, and 7.1 for DH 0, 2.5, and 5.0%, respectively. This shift in aggregation pH to higher pH values with increasing DH is similar to that found in the rheological experiments and during the visual observations described above.

Table 2. $pH_{Aggr-onset}$ at Various DH Values at $I = 0.03$, 0.2, and 0.5 M

DH value (%)	$pH_{Aggr-onset}$ $I = 0.03$	$pH_{Aggr-onset}$ $I = 0.2$	$pH_{Aggr-onset}$ $I = 0.5$
0	5.9	6.1	5.7
1.3	6.6	6.8	6.4
2.5	6.9	7.1	6.8
3.7	7.0	7.2	7.1
5.0	7.1	7.3	7.2
6.2	7.3	7.6	7.4[a]

[a] Already resulted in a clear gel after ionic strength was adjusted to 0.5M.

Table 3. Effect of Heating and Hydrolysis on the Hydrodynamic Diameter of SPI

sample	diameter[a] (nm)
nonheated SPI solution	131 ± 2
DH = 0%	197 ± 3
DH = 1.3%	137 ± 2
DH = 2.5%	137 ± 1
DH = 5.0%	176 ± 2
DH = 7.5%	413 ± 11
DH = 10.0%	1584 ± 353

[a] Errors represent the standard error of the cumulant fits within one measurement.

At higher ionic strengths similar turbidity patterns were observed as for $I = 0.03$ M, but some differences became apparent. At $I = 0.2$ and 0.5 M the maximum turbidities reached were around pH 4.2 and 3.7, respectively (**Figure 3**). Thereafter, at $I = 0.2$ M a slight decrease in turbidity was observed (**Figure 3**) below the pH of maximum turbidity, whereas at $I = 0.5$ M this decrease was absent (**Figure 3**).

Table 2 shows the $pH_{Aggr-onset}$ obtained for different DH values at all of the ionic strengths studied. These results show that the shift in $pH_{Aggr-onset}$ with increasing DH is on average the largest at $I = 0.2$, whereas at $I = 0.03$ and 0.5 M, the $pH_{Aggr-onset}$ is slightly lower.

The observed shift in $pH_{Aggr-onset}$ must be the result of the proteolytic activity of the subtilisin Carlsberg, because simultaneous addition of subtilisin Carlsberg and its inhibitor PMSF to the SPI solution at 40 °C resulted in turbidity patterns similar to those for the nonhydrolyzed SPI (no further data shown).

Aggregate Size. Heat and hydrolysis induced aggregation. This aggregate formation was studied by light scattering. **Table 3** shows the estimated average aggregate sizes obtained for the nonheated and heated SPI solution and hydrolysates at various DH values.

Heating the SPI solution resulted in the formation of aggregates, which was observed as a slightly opaque SPI solution. Upon hydrolysis a decrease in aggregate size was observed at DH = 1.3 and 2.5%, followed by a strong increase in aggregate size with a further increase in DH, as also observed by Ju and Kilara (*27*). As the estimated average size of the aggregates at DH 10% was found to be close to the limit of the apparatus, care should be taken with the interpretation of these results.

Protein and Peptide Size Distribution. HP-SEC was carried out to obtain an indication of the size of the peptides present in the SPI solution and the hydrolysates.

Figure 4 shows the HP-SEC chromatogram of the DH = 0, 2.5, and 5.0% samples. The chromatogram of DH = 0% contains five main peaks (fractions 1, 3, and 6−8) and two

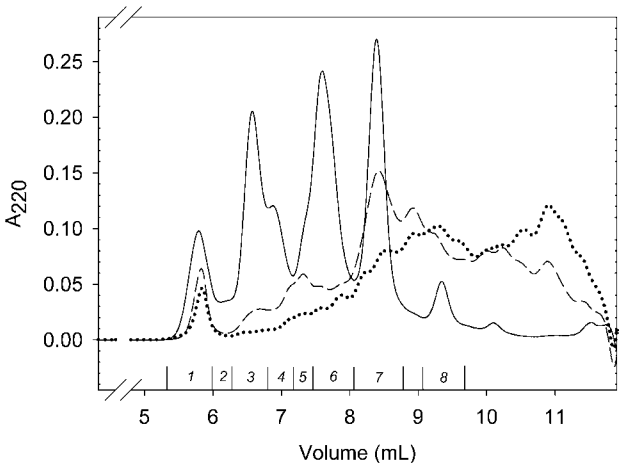

Figure 4. HP-SEC chromatogram of the DH = 0% (–), 2.5% (– –), and 5.0% (•••). Numbers 1–8 refer to fractions collected of the DH = 0% sample.

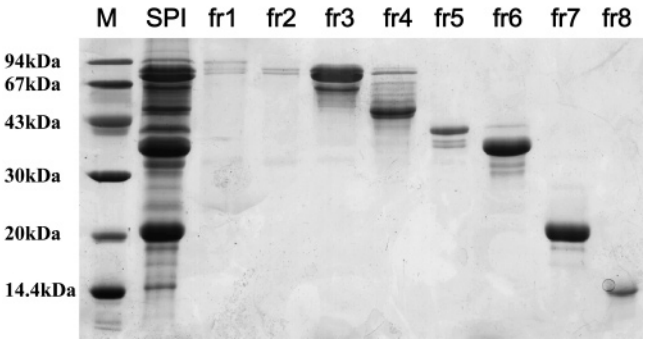

Figure 5. SDS-PAGE gel with the low molecular weight marker (M), the intact protein (SPI), and collected fractions 1–8 as indicated in the chromatogram of **Figure 4**.

shoulders (fractions 4 and 5). The fractions collected were analyzed by SDS-PAGE as shown in **Figure 5**, which also shows the protein composition of SPI. Fractions 1 and 2 elute around 5.7 mL, the void volume of the column, and therefore probably contain aggregates not dissociated by DTT and guanidinium. As can be observed in **Figure 4**, subtilisin Carlsberg was able to degrade the aggregates present in the first peak because the area of the peak decreased with increasing DH.

Figure 5 shows that fraction 3 contains several protein bands in the range of 55−70 kDa, probably representing the α-fraction of β-conglycinin. Fraction 4 shows a band around 50 kDa, which could be the β-fraction of β-conglycinin. A protein band around 36 kDa is present in fraction 5, representing the acid polypeptide A3 of glycinin. Fraction 6 has protein bands around 32 kDa, probably representing the acidic polypeptide of glycinin A1a, A2, A1b, and A4. Fraction 7 contains a band around 20 kDa, which probably consists of all the basic polypeptides of glycinin (*28*). In addition, the Kunitz inhibitor can be expected to be present. A protein band around 10 kDa can be observed in fraction 8, probably representing the acidic polypeptide A5 of glycinin.

The chromatograms in **Figure 4** clearly show that smaller fragments are formed with increasing DH and that already almost all of the intact protein has been degraded at DH = 2.5%. The SDS-PAGE gel in **Figure 6**, which shows the peptide patterns observed at various DH values, confirms this. Some new bands become apparent in the hydrolysates, which are not present in the nonhydrolyzed SPI solution, indicating that some

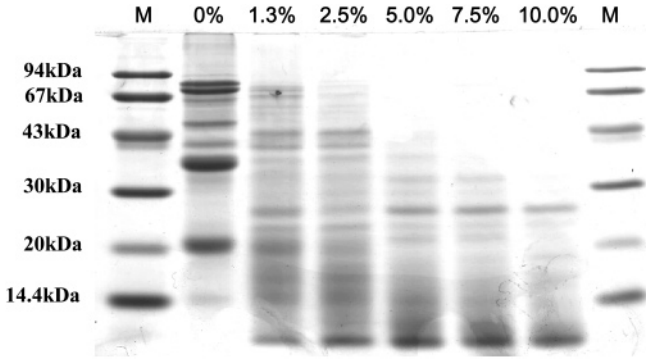

Figure 6. SDS-PAGE gel with the protein composition of different samples with increasing DH value (0, 1.3, 2.5, 5.0, 7.5, and 10.0%). The two outer lanes represent the marker (M).

more or less stable peptides are formed. In particular, the peptide with a molecular mass of ∼25 kDa seems to be quite resistant to enzymatic hydrolysis, as also reported by Inouye (*16*).

When the HP-SEC experiment was performed with samples prepared under nonreducing conditions, a minor shift to higher peptide sizes could be observed (data not shown). This was confirmed in an SDS-PAGE experiment under nonreducing conditions (data not shown). The minor shift to higher peptide size became less apparent with increasing DH.

DISCUSSION

Uncoupling of Hydrolysis and Gelation. In our experimental setup, the preparation of soy protein hydrolysate gels consisted of heating an SPI solution, followed by hydrolysis and finally acid-induced cold gelation in separate steps. A prerequisite for this approach is that gelation occurred only upon acidification. These conditions were met by, on the one hand, choosing a protein concentration not resulting in extensive aggregation or gelation upon heating and, on the other hand, by stopping the hydrolysis before visible aggregates were formed. This allowed hydrolysis and gelation to be studied separately. This approach is different from studies performed by, for example, Doucet et al. (*13*) and Otte et al. (*14*), in which gelation occurred already during the hydrolysis. The latter could therefore be defined as enzyme-induced gelation. Our approach is defined as acid-induced gelation of hydrolysates.

In our preparations enzyme-induced gelation also occurred, around an estimated DH of 10%, when hydrolysis was performed without stirring and pH control. This is what could be expected on the basis of the increase in aggregate size at DH = 10.0% (**Table 3**), as also reported by Inouye et al. (*16*). Because our aim was to uncouple the hydrolysis from the gelation, such high DH values were not studied in detail.

Shift in Aggregation and Gelling pH. The uncoupling of hydrolysis and gelation made it possible to study the effect of the pH on the gel formation. The rheological experiments showed that the higher the DH, the higher the pH at which gels could be formed. With the hydrolysates, gels could be made at pH values at which the nonhydrolyzed SPI did not yet form a gel. This makes the use of hydrolyzed SPI interesting for foods at neutral and slightly acidic pH. In addition, lower amounts of protein are needed when compared to heat-induced gels. The gels formed may also have a new texture that could be of interest of the food industry. Our results are in agreement with the observations of Ipsen et al. (*29*), who studied enzyme-induced gelation of whey protein systems at various pH values and found that at pH values further away from the p*I* of the parental protein, a higher DH was necessary to form a gel.

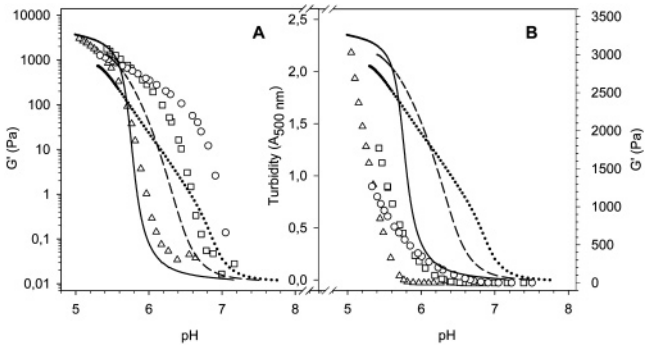

Figure 7. Development of the storage modulus (G') for DH = 0% (△), 2.5% (□), and 5.0% (○) and turbidity ($A_{500\ nm}$) for DH = 0% (–), 2.5% (– –), and 5.0% (•••) as a function of pH at $I = 0.03$ M, with the storage modulus on a logarithmic (**A**) and linear (**B**) scale.

When the shift in aggregation pH during acidification is studied, time scale effects have to be taken into account. These time scale effects can be observed clearly in **Figure 3** as the difference between the slow and fast acidification. The curves of gels prepared from the same hydrolysate at the same ionic strength do not overlap, due to the difference in acidification rate. The slower the acidification rate, the more time the proteins will spend at one particular pH to form aggregates, resulting in a higher turbidity at that pH. These time scale effects become even more apparent when data from measurements performed during acidification (rheological and turbidity measurements) are compared with data from experiments performed after the acidification had finished (visual observations and CSLM imaging). The DH = 5.0% ($I = 0.03$ M) hydrolysate had formed a gel at pH 7.6 after 16 h of incubation (**Table 1**), whereas no increase in turbidity was observed at pH 7.6 for this hydrolysate during acidification (**Figure 3**).

Rheological measurements are a useful tool to study the shift in aggregation pH, but they have the disadvantage that they are time-consuming and cannot be used in systems that show syneresis, as occurred at pH values below 5−5.5. Measurements that are less time-consuming and able to provide information about a broader pH range would therefore be more favorable. Turbidity experiments have the advantage that various samples can be measured in parallel, and by choosing a cuvette with a short light path, visible syneresis could in this case be prevented. These advantages enable measurements in a broader pH range. The turbidity measurements relate well with rheological experiments when G' is plotted on a logarithmic scale (**Figure 7A**) and can therefore be used to provide reliable indications about the gel formation of the preparations studied. When G' is plotted on a linear scale, it can be seen that aggregation, measured as increase in turbidity, precedes gelation, measured as the increase of G' (**Figure 7B**), as also observed by Alting et al. (*26*).

Proposed Mechanism of Peptide Aggregation. The gels formed from hydrolysates were not built up from intact soy proteins, because at DH values of 2.5% and higher, almost no intact soy proteins were present (**Figure 4**). This is what might be expected when 2.5% of the peptide bonds are cleaved. In addition, subtilisin Carlsberg has a broad specificity, but prefers to cleave next to neutral and acidic amino acids (*21*), so a broad spectrum of peptides can be expected. Some of these peptides are held together by disulfide bridges, but this effect seems to be minor. Part of the peptides form soluble aggregates during hydrolysis below a DH of 10%. These aggregates increase in diameter with increasing DH. Around DH = 10% insoluble aggregates are already formed during hydrolysis (**Table 3**). Upon acidification, the aggregates formed during hydrolysis might aggregate further with peptides or other aggregates. Because the shift in $pH_{Aggr-onset}$ increases with increasing DH, this shift is probably not the result of the release of some very specific peptides that accumulate with increasing DH.

Possible explanations for the shift in aggregation pH upon hydrolysis have been previously suggested in studies concerning the hydrolysis of whey proteins with Alcalase (*30*) or BLP (*31*). Part of the peptides formed were observed to have a higher p*I* (*31*, *32*) when compared to the parental protein. A change in p*I* changes the balance between electrostatic and hydrophobic forces and can thus result in aggregate formation around the p*I* of the peptides. The similarity between these observations with whey proteins and the observations made for soy proteins as presented here suggests a similar mechanism.

In general, the balance between electrostatic repulsion and hydrophobic attraction determines whether a protein forms aggregates or not. If this is the dominant mechanism in our gels, then at higher pH values aggregates are expected to be formed with increasing ionic strength, due to screening of the repulsive electrostatic forces, enabling the hydrophobic forces to dominate. In **Figure 3**, however, no large influence of the ionic strength can be observed on the $pH_{Aggr-onset}$. This indicates that the observed aggregation is not simply a balance of repulsive electrostatic and attractive hydrophobic interactions, but is more complex. Possibly also specific electrostatic attractions play a role, making the aggregation mechanism much more delicate and less predictable. Moreover, effects on aggregation kinetics may not become apparent within the time scale of the experiment. When a mixture of peptides is present with a wide variety of p*I* values, then at a certain pH, the peptides present will have a net charge that is either positive, negative, or zero. This might lead to aggregation due to hydrophobic attraction of peptides with a net charge of zero, whereas electrostatic attraction takes place between oppositely charged peptides. In addition to these interactions, also peptides with a high polarity or hydrophobicity may be formed that will or will not form aggregates, independent of the pH.

We are currently investigating whether the aggregation behavior is as complex and nonspecific as described above. The focus in future research will be on characterization of the peptides that participate in the gel network.

ACKNOWLEDGMENT

We thank Saskia de Jong and Jan Klok from NIZO food research for assisting with the rheology and CSLM experiments, respectively. The soybeans were kindly provided by Fa. L. I. Frank (Twello, The Netherlands).

LITERATURE CITED

(1) Utsumi, S.; Kinsella, J. E. Forces involved in soy protein gelation—Effects of various reagents on the formation, hardness and solubility of heat-induced gels made from 7S, 11S, and soy isolate. *J. Food Sci.* **1985**, *50*, 1278−1282.

(2) Renkema, J. M. S.; Gruppen, H.; van Vliet, T. Influence of pH and ionic strength on heat-induced formation and rheological properties of soy protein gels in relation to denaturation and their protein compositions. *J. Agric. Food Chem.* **2002**, *50*, 6064−6071.

(3) Renkema, J. M. S.; van Vliet, T. Heat-induced gel formation by soy proteins at neutral pH. *J. Agric. Food Chem.* **2002**, *50*, 1569−1573.

(4) Bryant, C. M.; McClements, D. J. Molecular basis of protein functionality with special consideration of cold-set gels derived from heat-denatured whey. *Trends Food Sci. Technol.* **1998**, *9*, 143−151.

(5) Kohyama, K.; Nishinari, K. The effect of glucono-δ-lactone on the gelation time of soybean 11S protein: Concentration dependence. *Food Hydrocolloids* **1992**, *6*, 263−274.
(6) Damodaran, S. Amino acids, peptides, and proteins. In *Food Chemistry*; Fennema, O. R., Ed.; Dekker: New York, 1996; pp 322−429.
(7) Doi, E. Gels and gelling of globular proteins. *Trends Food Sci. Technol.* **1993**, *4*, 1−5.
(8) Kruif de, C. G. Skim milk acidification. *J. Colloid Interface Sci.* **1997**, *185*, 19−25.
(9) Panyam, D.; Kilara, A. Enhancing the functionality of food proteins by enzymatic modification. *Trends Food Sci. Technol.* **1996**, *7*, 120−125.
(10) Nielsen, P. M. Functionality of protein hydrolysates. In *Food Proteins and their Applications*; Damodaran, S., Paraf, A., Eds.; Dekker: New York, 1997; pp 443−472.
(11) Ju, Z. Y.; Otte, J.; Madsen, J. S.; Qvist, B. Effects of limited proteolysis on gelation and gel properties of whey protein isolate. *J. Dairy Sci* **1995**, *78*, 2119−2128.
(12) Fuke, Y.; Sekiguchi, M.; Msuoka, H. Nature of stem bromelain treatments on the aggregation and gelation of soybean proteins. *J. Food Sci.* **1985**, *50*, 1283−1288.
(13) Doucet, D.; Gauthier, S. F.; Foegeding, E. A. Rheological characterization of a gel formed during extensive enzymatic hydrolysis. *J. Food Sci.* **2001**, *66*, 711−715.
(14) Otte, J.; Ju, Z. Y.; Faergemand, M.; Lomholt, S. B.; Qvist, K. B. Protease-induced aggregation and gelation of whey proteins. *J. Food Sci.* **1996**, *61*, 911−923.
(15) Murata, K.; Kusakabe, I.; Kobayashi, H.; Kiuchi, H.; Murakami, K. Selection of commercial enzymes suitable for making soymilk-curd. *Agric. Biol. Chem.* **1987**, *51*, 2929−2933.
(16) Inouye, K.; Nagai, K.; Takita, T. Coagulation of soy protein isolates induced by subtilisin Carlsberg. *J. Agric. Food Chem.* **2002**, *50*, 1237−1242.
(17) Ottesen, M.; Svendsen, A. The subtilisins. *Methods Enzymol.* **1970**, *19*, 199−215.
(18) Morr, C. V. Recalculated nitrogen conversion factors for several soybean protein products. *J. Food Sci.* **1982**, *47*, 1751−1752.
(19) Hermansson, A.-M. Physico-chemical aspects of soy proteins structure formation. *J. Texture Stud.* **1978**, *9*, 33−58.
(20) Adler-Nissen, J. *Enzymic Hydrolysis of Food Proteins*; Elsevier Applied Science Publishers: London, U.K., 1986; 427 pp.
(21) Beynon, R.; Bond, J. S. *Proteolytic Enzymes*, 2nd ed.; Oxford University Press: Oxford, U.K., 2001; 340 pp.
(22) James, G. T. Inactivation of the protease inhibitor phenylmethylsulfonyl fluoride in buffers. *Anal. Biochem.* **1978**, *86*, 574−579.
(23) Alting, A. C.; de Jongh, H. H. J.; Visschers, R. W.; Simons, J. Physical and chemical interactions in cold gelation of food proteins. *J. Agric. Food Chem.* **2002**, *50*, 4682−4689.
(24) Hoffmann, M. A. M.; Roefs, S.; Verheul, M.; VanMil, P.; DeKruif, K. G. Aggregation of β-lactoglobulin studied by in situ light scattering. *J. Dairy Res.* **1996**, *63*, 423−440.
(25) Walstra, P. Soft Solids. In *Physical Chemistry of Foods*; Walstra, P., Ed.; Dekker: New York, 2003; pp 683−771.
(26) Alting, A. C.; Weijers, M.; De Hoog, E. H. A.; van de Pijpekamp, A. M.; Stuart, M. A. C.; Hamer, R. J.; De Kruif, C. G.; Visschers, R. W. Acid-induced cold gelation of globular proteins: Effects of protein aggregate characteristics and disulfide bonding on rheological properties. *J. Agric. Food Chem.* **2004**, *52*, 623−631.
(27) Ju, Z. Y.; Kilara, A. Gelation of hydrolysates of a whey protein isolate induced by heat, protease, salts and acid. *Int. Dairy J.* **1998**, *8*, 303−309.
(28) Utsumi, S.; Matsumura, Y.; Mori, T. Structure−function relationships of soy proteins. In *Food Proteins and their Applications*; Damodaran, S., Praf, A., Eds.; Dekker: New York, 1997; pp 257−291.
(29) Ipsen, R.; Otte, J.; Lomholt, S. B.; Qvist, K. B. Standardized reaction times used to describe the mechanism of enzyme-induced gelation in whey protein systems. *J. Dairy Res.* **2000**, *67*, 403−413.
(30) Doucet, D.; Otter, D. E.; Gauthier, S. F.; Foegeding, E. A. Enzyme-induced gelation of extensively hydrolyzed whey proteins by Alcalase: Peptide identification and determination of enzyme specificity. *J. Agric. Food Chem.* **2003**, *51*, 6300−6308.
(31) Otte, J.; Lomholt, S. B.; Ipsen, R.; Stapelfeldt, H.; Bukrinsky, J. T.; Qvist, K. B. Aggregate formation during hydrolysis of beta-lactoglobulin with a Glu and Asp specific protease from *Bacillus licheniformis*. *J. Agric. Food Chem.* **1997**, *45*, 4889−4896.
(32) Doucet, D.; Gauthier, S. F.; Otter, D. E.; Foegeding, E. A. Enzyme-induced gelation of extensively hydrolyzed whey proteins by Alcalase: Comparison with the plastein reaction and characterization of interactions. *J. Agric. Food Chem.* **2003**, *51*, 6036−6042.

Received for review August 18, 2004. Revised manuscript received November 5, 2004. Accepted November 24, 2004. The research in this paper was supported by The Graduate School VLAG.

JF048622H